Intelligent and Sustainable Manufacturing

SCIEPublish

Article

Geometric Characterization and Prediction of Tool Wear in Ultrasonic Machining Using Reverse Engineering and Machine Learning

Arindam Chakraborty [1], Kailash Roy [2], Sudip Santra [1,*], Biswanath Doloi [1], Somnath Das [3] and Jitendra Sarkar [4]

[1] Production Engineering Department, Jadavpur University, Kolkata 700032, India; arindamckbt@gmail.com (A.C.); bdoloionline@rediffmail.com (B.D.)
[2] Mechanical Engineering Department, IIT Kanpur, Kanpur 208016, India; kailashroy07@gmail.com (K.R.)
[3] Department of Mechanical Engineering, Swami Vivekananda Institute of Science & Technology, Kolkata 700145, India; somnath96@gmail.com (S.D.)
[4] Mechanical Engineering Department, Brainware University, Kolkata 700125, India; jitendrasarkar2009@gmail.com (J.S.)

* Corresponding author. E-mail: sudip16santra@gmail.com (S.S.)

Received: 1 October 2026; Revised: 12 October 2026; Accepted: 5 November 2026; Available online: 9 November 2026

ABSTRACT: The ultrasonic machining product depends heavily on tool shape, as the tool replicates the workpiece surface. Because of this, tool wear during ultrasonic machining (USM) needs in-depth analysis, as it changes tool geometry and can affect the dimensions of the machined cavity. This study examines an image-based reverse-engineering workflow for characterizing changes in USM tool geometry over cumulative machining time. Images captured using a digital microscope were processed to obtain three-dimensional point-cloud data, from which tool height, width, and volume were evaluated. Linear Regression (LR), Random Forest Regression (RFR), and Extreme Gradient Boosting (XGBoost) were used to estimate the measured geometric responses. The recorded measurements showed an overall reduction in tool dimensions and volume during the experimental sequence. The model estimates followed the broad trends in the data, although their agreement varied by response and machining stage. The work demonstrates the use of microscope-based image capture and point-cloud processing for tracking tool geometry and provides an initial comparison of regression approaches for the recorded sequence.

Keywords: Tool wear; Ultrasonic machining; Reverse engineering; CAD model; Machine learning (ML)

1. Introduction

Ultrasonic machining (USM) is a non-traditional machining process used to machine hard and brittle materials. In this process, the tool vibrates at an ultrasonic frequency with a small amplitude while abrasive particles suspended in a slurry repeatedly impact the workpiece. These impacts initiate and extend microcracks near the surface, contributing to material removal. The process is useful where conventional machining may cause excessive forces or damage to brittle materials.

Reverse engineering (RE) involves acquiring geometric information from a physical component and using it to construct a digital representation. In this study, a microscope-based image-capture arrangement

© 2026 The authors. This is an open access article under the Creative Commons Attribution 4.0 International License (https://creativecommons.org/licenses/by/4.0/).

was used to record changes in tool geometry during machining. The approach allowed the tool profile to be examined at successive stages without contacting the measured surface.

Ultrasonic machining (USM) is an effective non-conventional machining process for fabricating micro-features in hard and brittle materials. However, Mirad et al. [1] documented that tool wear remains a major limitation affecting dimensional accuracy, surface quality, and machining efficiency. To overcome these limitations, Kumar et al. [2] introduced rotary tool micro-USM (RT-MUSM), demonstrating improved abrasive slurry replenishment, reduced tool wear, and enhanced microchannel form accuracy. Kumar et al. [3,4] established that tungsten carbide tools exhibited superior wear resistance compared with SS-304 tools, resulting in improved machining performance. Ultrasonic machining (USM) has emerged as an effective non-conventional machining process for fabricating intricate features in hard, brittle, and composite materials. Asmael et al. [5] reviewed the applications of USM in carbon fibre-reinforced polymer composites, highlighting its potential for improving surface quality while reducing delamination and fibre fracture. Yu et al. [6] identified low-cycle fatigue as the dominant mechanism responsible for tool wear in micro-USM and developed a theoretical model for its prediction. Wang et al. [7] investigated the relationship between tool wear and material removal using numerical simulations and experiments, demonstrating the influence of tool material properties on machining efficiency.

Das et al. [8] used reverse engineering to develop a hemispherical USM tool for machining zirconia. Ferreira et al. [9] combined rapid tooling and reverse engineering to produce EDM electrodes from a wax prototype. Valerga et al. [10] reconstructed milling tools using three-dimensional scanning and fused deposition modelling, reporting geometries close to the original tools. Other studies have applied reverse engineering to tool-wear assessment and simulation [11,12]. Kyaw et al. [13] compared photogrammetry, laser scanning, and three-dimensional modelling in the remanufacturing of automotive components.

Despite these developments, acquiring complete geometric information and converting measured surfaces into useful digital models remain challenging, particularly for components with complex profiles [14]. Reverse engineering is used in applications such as component reconstruction when design documentation is unavailable, reproduction of spare parts, and repair of damaged components [15]. For tool-wear studies, it also provides a means of comparing geometry at different stages of operation [16].

Conventional cutting processes can be difficult to apply to hard and brittle materials because of the high forces and stresses involved [17]. Ultrasonic Machining (USM) is therefore used for materials such as ceramics, carbides, composites, and other brittle workpieces [18]. Material removal in USM is associated with repeated abrasive impacts and the cracks formed near the workpiece surface [19]. Mirad and Das [20] used support vector regression to estimate tool wear during USM of Inconel 718, reporting improved predictive performance when acoustic-emission features were included alongside process information.

Although USM can produce complex cavities in brittle materials, the tool geometry changes during operation and may influence the resulting cavity profile. Previous studies have examined reverse engineering for tool reconstruction and machine-learning methods to estimate machining behaviour. The present study combines image-based 3D CAD model generation with regression modelling to examine the changes in volume, tool height, and width during a cumulative machining over time.

The objective of this study was to capture changes in USM tool geometry during machining of a metal-matrix-composite (MMC) workpiece and to predict the tool geometry using machine-learning models. An image-based point-data cloud was used to generate 3D CAD models to evaluate volume, tool height, and width. Linear Regression, Random Forest Regression, and XGBoost were the selected machine learning models.

2. Materials and Methods

The experimental work comprised ultrasonic machining, image capture of the tool before and after machining, processing of the captured images, and analysis of the resulting geometric data. The workpiece

material and abrasive slurry were prepared for the machining trials, and the measured tool geometry was compared across the cumulative machining time.

2.1. Machining Setup and Planning

The experiments were performed using a Sonic-Mill AP-100 ultrasonic machining machine, manufactured by Sonic-Mill, USA, and installed at Jadavpur University, Kolkata, India under the process conditions listed in Table 1. The operating frequency and amplitude were maintained at 20 kHz and 0.25 µm, respectively, during the complete machining process. A Box–Behnken design was adopted to generate the parametric combinations. Power rating, abrasive-slurry concentration, and slurry-flow rate were the varied process parameters. The values of power ratings, abrasive-slurry concentrations, and slurry-flow rates are specified in Table 1. Tool geometry was recorded after successive every machining to study dimensional changes during operation.

Table 1. Process Parameters for USM Machining.

Exp. No.	Power Rating (W)	Abrasive Slurry Concentration (wt %)	Abrasive Slurry Flow Rate (mL/s)
1	250	15	75
2	300	25	50
3	200	25	50
4	250	25	25
5	200	20	75
6	300	20	75
7	250	20	50
8	300	20	25
9	200	20	25
10	200	25	50
11	300	25	50
12	250	25	75
13	250	25	25

2.2. Material

The workpiece selected was an MMC made of A356 aluminium alloy (71.11 wt%) as the base matrix. The nominal composition of the material is given in Table 2. The composition of the Al-based metal matrix composite is shown in Figure 1a, and the XRD plot is shown in Figure 1b. High-purity magnesium ingots (99.9%) were used for the additional magnesium charge intended to promote Mg_2Si formation. The silicon carbide crucible was preheated to 600 °C for 30 min to remove residual moisture. The A356 alloy was melted at 750 ± 10 °C, with the charge preheated to 200 °C before loading to reduce thermal shock. After complete melting, the melt was held for 15 min for temperature equilibration, and surface oxides were removed using preheated skimming tools. The melt temperature was then adjusted to700 ± 5℃. Magnesium was introduced below the melt surface in increments of 50–100 g, and the melt was maintained at 660–680 °C for 20–30 min to promote the reaction $2Mg + Si \rightarrow Mg_2Si$. The melt was skimmed again and brought to the casting temperature, followed by a 10 min stabilization period. The final magnesium content and resulting phase composition should be reported from the batch record or material analysis if available.

Table 2. Compositions of the Al-based MMCs.

Elements	Weight Percentage
Silicon (Si)	15.11
Iron (Fe)	0.67
Magnesium (Mg)	4.15

Oxygen (O)	8.94
Aluminium (Al)	71.11

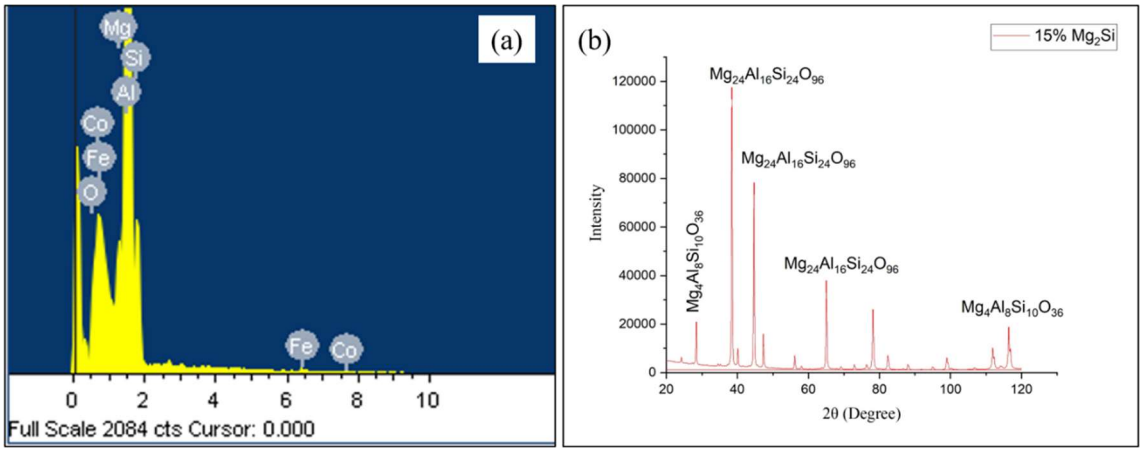


Figure 1. (**a**) Al-based MMCs' EDS picture and (**b**) the material's XRD plot.

2.3. Data Extraction and Processing Methodology

Tool geometry was measured using a Dyno digital microscope at 40× magnification. Before measurements, the microscope was calibrated at 40× using the 1 mm reference scale supplied with the instrument. The maximum dimensions of tool height and width were measured before and after the experiment to constrain and generate the point data cloud. This is important, if we skip this step, then the generated point-data cloud would not yield true dimension of the tool. The captured images were processed using a Python-based program to obtain three-dimensional point-cloud coordinates (X, Y, Z), which were subsequently processed in Geomagic Design X (version 2016.2.0) for generation 3D CAD model of the tool. Figure 2 shows an overall flow chart of the entire workflow. The Geomagic Design X software was used for generation of the 3D CAD model and obtaining the volume of the generated CAD model.

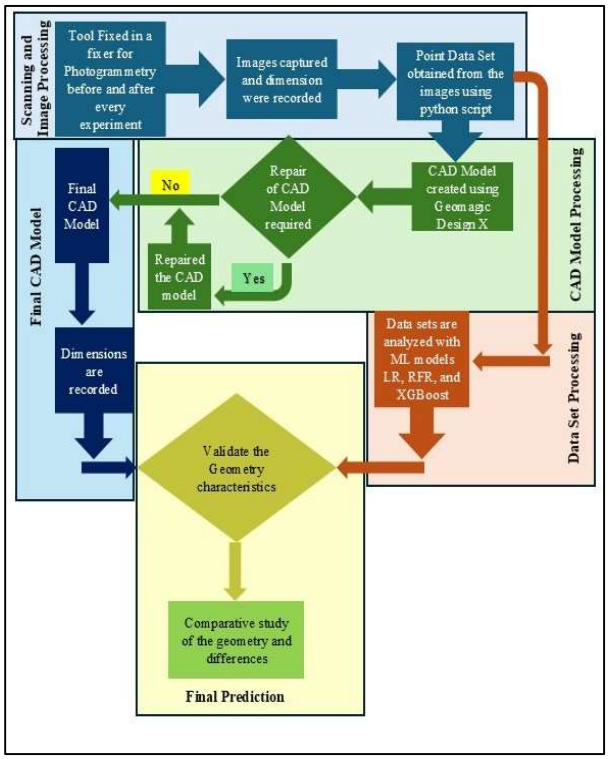


Figure 2. The flow process of the study.

The generated CAD models were analyzed using three regression based Machine Learning models: Linear Regression (LR), Random Forest Regression (RFR), and Extreme Gradient Boosting (XGBoost). LR was used as a baseline model, while RFR and XGBoost were included to represent potentially nonlinear relationships between the input variables and the measured responses. Predicted and recorded values of tool volume, height, and width were compared across all ML models.

2.4. Photogrammetry-Based Image Capture Setup

The selected tool had a triangular cross-section and was held in a custom wooden fixture, as shown in Figure 3. The fixture helped maintain a consistent position during image capture. To make measurement easier under the microscope, a reference line was drawn on the tool to indicate the area of interest. Images were captured at the subsequent machining.

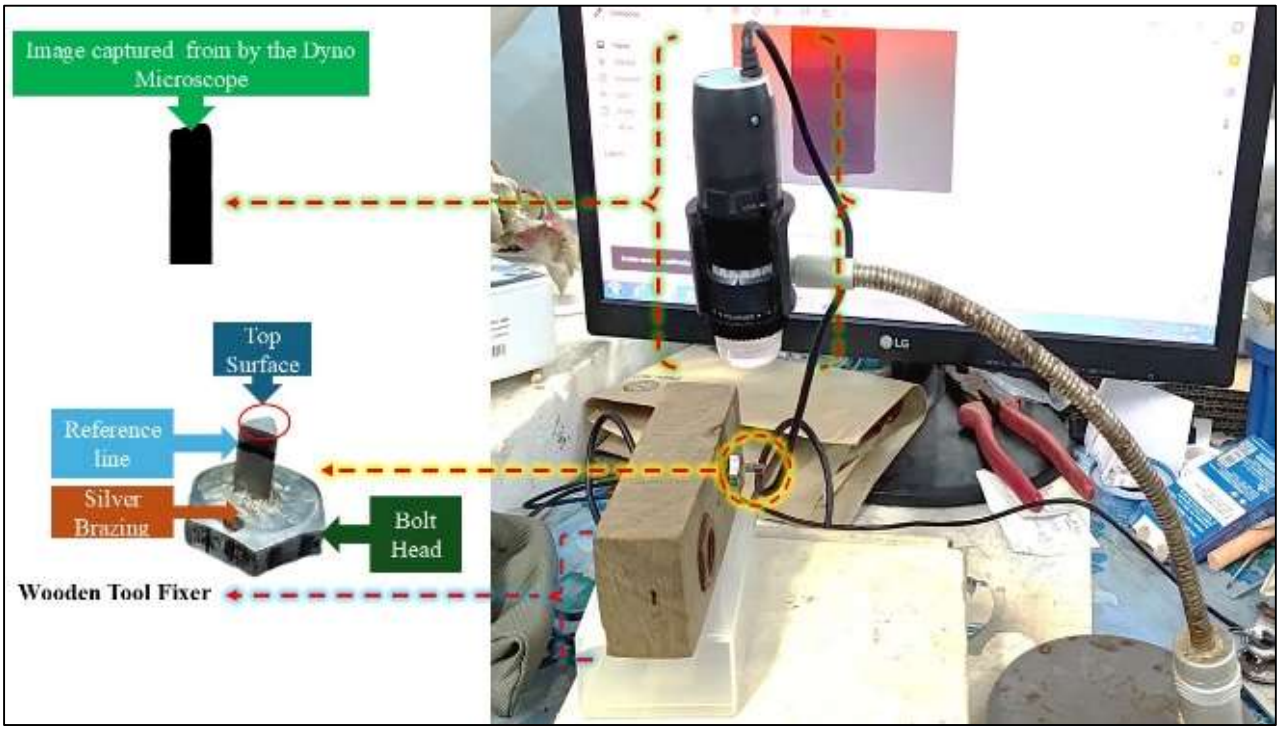


Figure 3. Image capture setup.

2.5. Image Data Extraction and Processing

The captured images were processed to generate three-dimensional point-cloud data using a python based program developed in-house. The data generated from the program was used to construct a 3D CAD model of the tool. The CAD models were further analyzed and extract various geometric features considered of the tool. The obtained values were compared across all machining stages to study changes in tool dimensions and volume.

3. Tool Wear Mechanism in Ultrasonic Machining

Tool wear in Ultrasonic Machining (USM) resulted from repeated impacts, abrasion, erosion, and fatigue caused by abrasive particles moving between the vibrating tool and the workpiece. The tool vibrates at an ultrasonic frequency, generally around 20 kHz, with a small amplitude of 0.25 µm. Although the primary purpose of the abrasive particles was to remove material from the workpiece, some particles also interacted with the tool surface, resulting in gradual material loss and changes in tool geometry.

Impact-induced fatigue wear occurred when repeated abrasive particle impact generated cyclic stresses on the tool surface. Over time, these stresses caused surface fatigue, crack initiation, crack propagation, and detachment of small fragments from the tool. Erosive wear happened during machining, where abrasive particles repeatedly strike the tool surface and remove small amounts of material. This impact-driven erosion caused pitting, surface roughening, edge chipping, lateral cracking, and progressive degradation of the tool tip. A tool material with high resistance against wear and scratches reduces tool wear and increases tool life. Higher vibration amplitude would increase the kinetic energy of the particles and intensify erosive wear. Process parameters also affected tool wear, including vibration amplitude, static load, abrasive grain size, abrasive concentration, machining time, and tool material. Increasing abrasive concentration intensified abrasive impacts, resulting in reduced tool life. Tool hardness, toughness, flexibility, and work-hardening behaviour may also influence wear resistance.

4. Results & Discussions

Tool height and width were recorded before and after every machining, as listed in Table 3. Figure 4 presents the measured dimensional trends with cumulative machining time. Both dimensions decreased overall, although the magnitude of the difference differed between the height and width measurements.

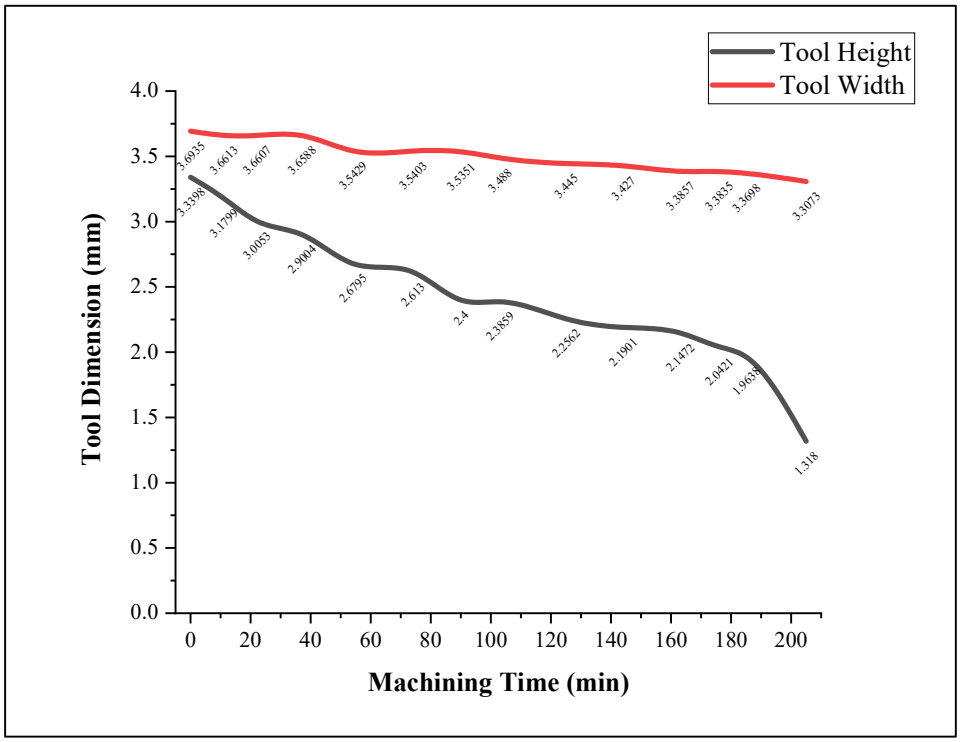


Figure 4. Changes in the geometry of the tool with the machining time.

Table 3. Geometric parameters for the process parameters.

Exp. No.	Power Rating (W)	Abrasive Slurry Concentration (wt %)	Abrasive Slurry Flow Rate (mL/s)	Cumulative Machining Time (min)	Tool Height (mm)	Tool Width (mm)
1	250	15	75	11	3.1799	3.6613
2	300	25	50	22	3.0053	3.6607
3	200	25	50	37	2.9004	3.6588
4	250	25	25	54	2.6795	3.5429
5	200	20	75	74	2.613	3.5403
6	300	20	75	90	2.4	3.5351
7	250	20	50	103	2.3859	3.488

8	300	20	25	125	2.2562	3.445
9	200	20	25	144	2.1901	3.427
10	200	25	50	163	2.1472	3.3857
11	300	25	50	176	2.0421	3.3835
12	250	25	75	185	1.9638	3.3698
13	250	25	25	205	1.318	3.3073

4.1. Experimental and Predicted Tool Geometry

Point-cloud data were used to generate a digital 3D CAD model of the tool at each recorded machining stage, and the corresponding volume estimates are listed in Table 4. The measured volume also decreased overall as machining time increased, due to a decrease in tool height and width shown in Figures 5 and 6. Tool wear in ultrasonic machining (USM) was significantly influenced by power rating, slurry concentration, and slurry flow rate. Increasing power rating generally intensified abrasive particle impacts, leading to increased tool wear through abrasion, erosion, and fatigue. Increasing slurry concentration increased the number of abrasive particles interacting with the tool at an instance, which accelerated tool wear; however, excessive concentration restricted particle movement and reduced machining efficiency. Slurry flow rate affected abrasive replenishment and debris removal; an excessively high flow rate intensified erosive wear, whereas insufficient flow caused debris accumulation and unstable machining. The reduction was not uniform across the sequence, indicating that the measured volume changed at different rates during the experiment. The observed variations may be attributed to different process parameters during cumulative machining. Since this study focused on CAD model reconstruction and tool wear prediction rather than parameter optimization, a linear or smooth trend was not necessarily expected.

Table 4. Tool volume from the point cloud.

Cumulative Machining Time (min)	Actual Volume (mm^3)	Linear Regression Predicted Volume (mm^3)	Random Forest Predicted Volume (mm^3)	XGBoost Predicted Volume (mm^3)
0	18.5108	20.120	17.916	18.961
11	17.4638	18.977	18.219	18.961
22	16.5022	17.733	17.376	17.730
37	15.9179	17.076	17.203	17.107
54	14.2398	15.822	15.615	15.826
74	14.2061	14.297	14.506	14.284
90	12.7263	13.106	13.030	13.074
103	12.5275	12.570	12.551	12.608
125	11.6764	11.635	11.423	11.603
144	11.2582	11.218	11.190	10.675
163	11.0639	10.654	10.619	10.675
176	10.6241	10.201	10.458	9.753
185	10.0305	9.757	10.326	9.753
205	6.5385	6.421	7.921	6.425

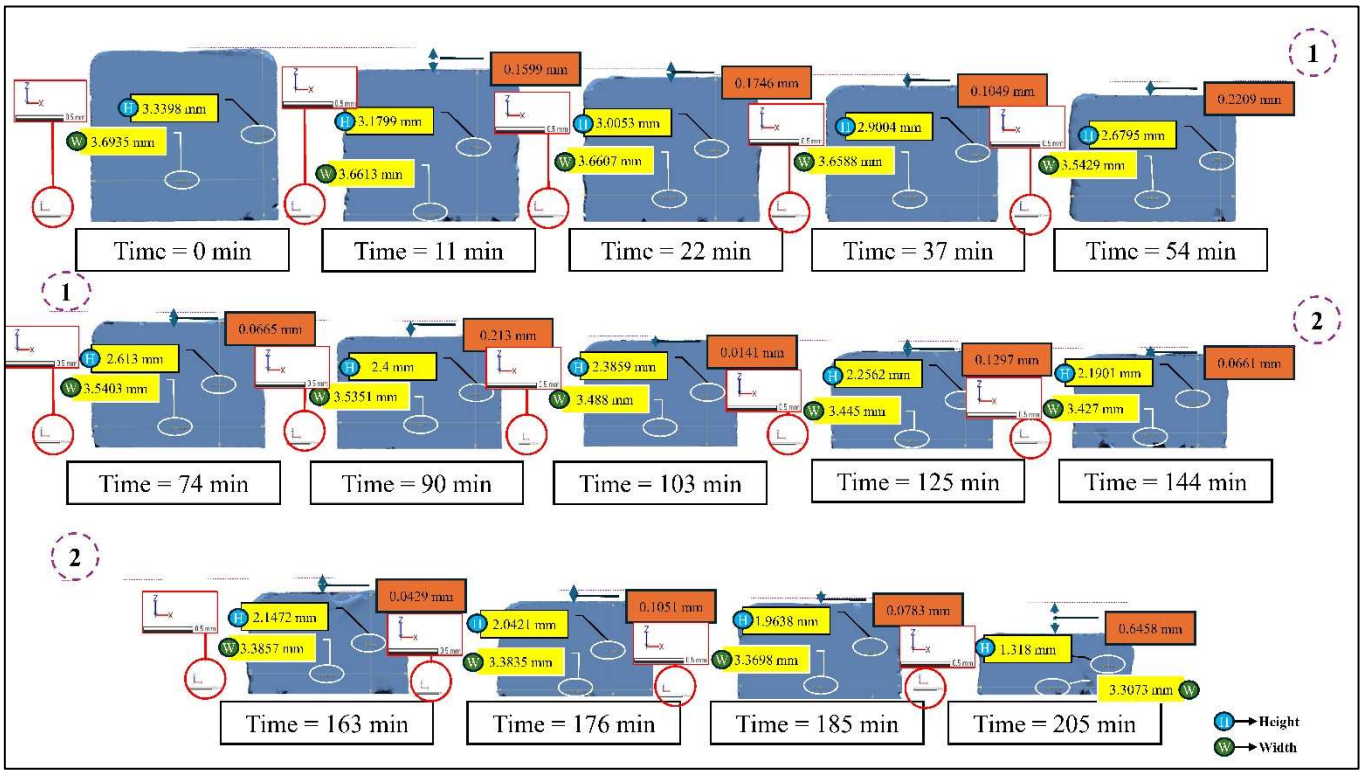


Figure 5. Change in USM tool height at cumulative machining time. Captions 1 and 2 indicate the measurement locations used to assess dimensions.

The height estimate followed a downward trend in the recorded measurements, although agreement varied among models throughout all machining stages. The machine learning analysis used process parameters such as machining time, power rating, abrasive slurry concentration, and slurry flow rate to predict changes in tool height, width, and volume. Models like Linear Regression (LR), Random Forest Regression (RFR), and Extreme Gradient Boosting (XGBoost) were implemented with specific hyperparameter settings. The input variables were retrained without the feature selection procedure. The analysis was validated by performing three experiments, and the changes were compared with the actual analysis to validate the cause. The model was evaluated manually and compared with experimentally measured values across the machining stages and assessed using RMSE and R^2. (Add all the train/test splits, cross-validation, hyperparameter settings, feature selection details HERE). For machining volume change (RMSE: 0.7524, R^2: 0.9324) and change in tool width variation (RMSE: 0.0384, R^2: 0.8894), Random Forest showed the greatest predictive performance; for cumulative change in tool height loss (RMSE: 0.0494, R^2: 0.9904), Linear Regression performed the best. Overall, no single approach consistently outperformed the others, and model performance varied among target parameters.

The predicted tool-height and tool-width values are summarized in Table 5. These estimates correspond to the recorded cumulative machining times and can be compared with the measured dimensions reported in Table 3.

Table 5. Predicted change in Tool height and width.

Cumulative Machining Time (min)	Linear Regression Predicted Change in Tool Height (mm)	Random Forest Predicted Change in Tool Height (mm)	XGBoost Predicted Change in Tool Height (mm)	Linear Regression Predicted Change in Tool Width (mm)	Random Forest Predicted Change in Tool Width (mm)	XGBoost Predicted Change in Tool Width (mm)
0	0	0	0	0	0	0
11	0.213	0.340	0.214	0.009	0.031	0.010
22	0.402	0.471	0.401	0.017	0.040	0.017
37	0.484	0.507	0.484	0.033	0.035	0.032
54	0.702	0.713	0.702	0.035	0.058	0.035
74	0.796	0.808	0.796	0.153	0.143	0.152
90	0.976	1.001	0.976	0.183	0.199	0.182
103	0.986	0.963	0.985	0.238	0.225	0.237
125	1.136	1.208	1.135	0.276	0.278	0.275
144	1.163	1.214	1.146	0.143	0.281	0.280
163	1.259	1.260	1.258	0.308	0.299	0.307
176	1.327	1.270	1.418	0.269	0.303	0.335
185	1.418	1.250	1.418	0.336	0.302	0.335
205	2.071	1.760	2.069	0.356	0.327	0.354

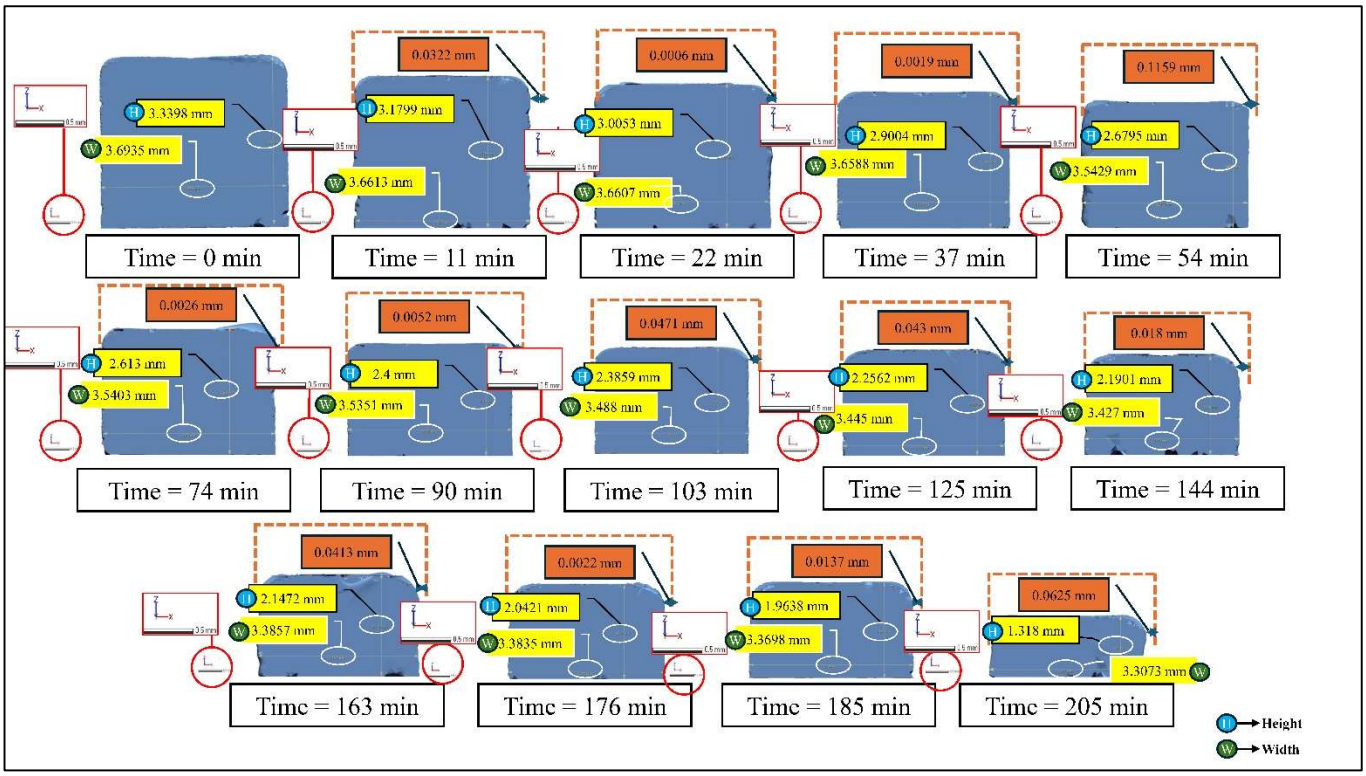


Figure 6. Change in USM tool width at cumulative machining time.

After 205 min of cumulative machining, the experimental results demonstrate a decrease in tool height from 3.3398 mm to 1.3180 mm. The best results were shown by Linear Regression (MAE: 0.0464 mm, RMSE: 0.0494 mm, R^2: 0.9904), followed by Random Forest (MAE: 0.0974 mm, RMSE: 0.1174 mm, R^2: 0.9404) and XGBoost (MAE: 0.0524 mm, RMSE: 0.0584 mm, R^2: 0.9854). The cumulative machining time method, in which several machining parameters were introduced one after the other, may be the cause of the significant differences in individual forecasts. Prediction disparities occurred because the models did

not fully account for the cumulative effects of previous machining conditions, which require more experiments and studies to understand thoroughly. However, the overall increasing trend of cumulative tool height loss with machining time was effectively reflected by all three models as shown in Figure 7.

Progressive lateral tool wear was evident as the experimental tool width dropped from 3.6613 mm to 3.3073 mm. The best results were obtained by Random Forest (MAE: 0.0334 mm, RMSE: 0.0384 mm, R^2: 0.8894), followed by Linear Regression (MAE: 0.0374 mm, RMSE: 0.0484 mm, R^2: 0.8254) and XGBoost (MAE: 0.0354 mm, RMSE: 0.0424 mm, R^2: 0.8674). The cumulative machining history may also be the cause of the prediction deviations, since changes in power rating, slurry concentration, and flow rate affected the continuous process rather than operating separately during training of the data set for all 3 ML models. More studies and experiments would provide further insight into the causes of these deviations. All three models replicated the overall increasing trend of tool width loss with machining time as shown in Figure 8, indicating their ability to describe general wear behavior, even though they could not fully capture these cumulative interactions.

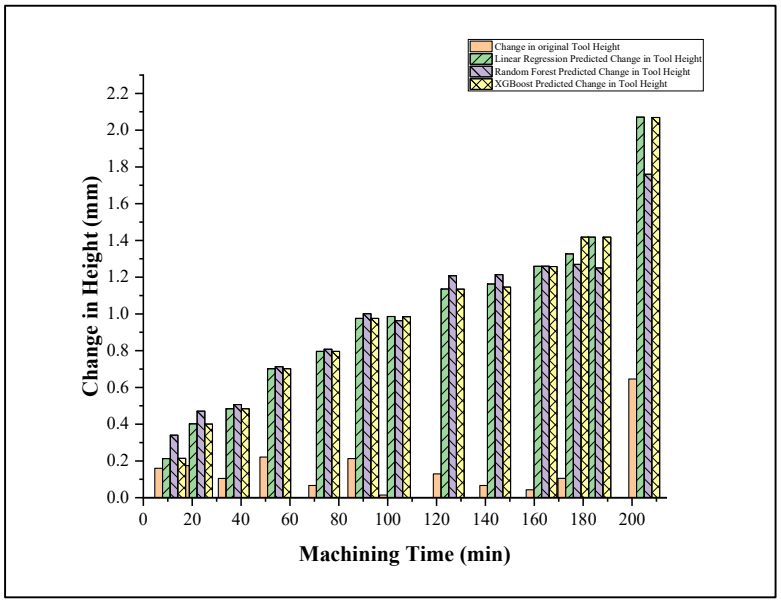


Figure 7. Prediction of the USM tool height wear.

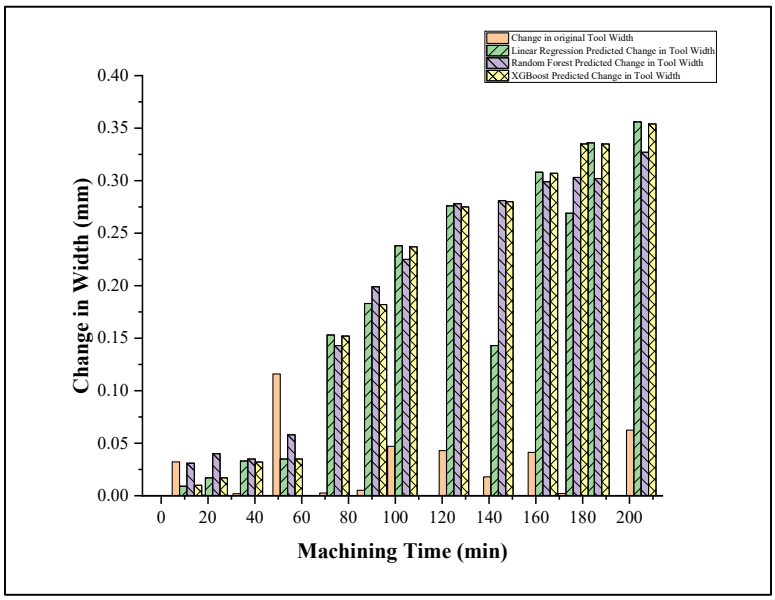


Figure 8. Prediction of the USM Tool width wear of the tool.

4.2. Verification of Tool-Wear Trend

The total machining times for the validation sequence were 11 and 74 min. The first machining stage was carried out at 250 W power, 15 wt% abrasive slurry concentration, and 75 mL/s flow rate, with a cumulative machining time of 11 min. The second experimental condition was carried out at 200 W, 20 wt% concentration, and 75 mL/s flow rate, with a cumulative machining time of 74 min. The two parameters selected for validation are essentially the first and fifth experimental parameters of Table 3. Tool geometry was measured using the same image-based procedure as in the main sequence, and the results were compared to assess whether the dimensional trend was consistent across these selected stages.

The 3D CAD model for the selected stages is shown in Figure 9. The measured tool height was 3.3398 mm at 0 min, 3.1799 mm at 11 min, and 2.6313 mm at 74 min. The height decreased by 0.1599 mm from 0 to 11 min and by 0.5486 mm from 11 to 74 min, for a total reduction of 0.7085 mm between the initial condition and 74 min.

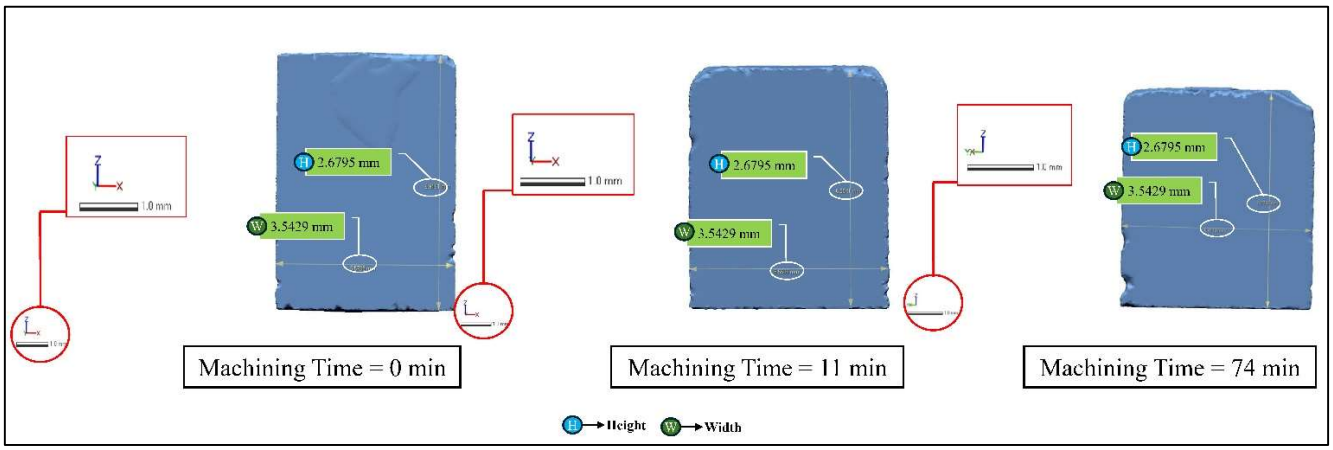


Figure 9. 3D CAD models comparing the USM tool geometry before and after experimental validation.

The measured width decreased by 0.0222 mm from 0 to 11 min and by 0.1450 mm from 11 to 74 min. The total reduction over the selected sequence was 0.1672 mm. The larger change during the 11 to 74 min interval indicates that the measured lateral dimension changed more over that part of the sequence as stated in the Table 6.

Table 6. Verification results for USM tool height and width.

ML Model	Cumulative Time (min)	Tool Height (mm)		Tool Width (mm)	
		Measured	Predicted	Measured	Predicted
Initial Condition	0	3.3398	3.3398	5.5785	5.5785
Linear Regression	11	3.1799	3.0932	5.5563	5.5827
	74	2.6313	2.6316	5.4113	5.4691
Random Forest	11	3.1799	3.0824	5.5563	5.5779
	74	2.6313	2.5611	5.4113	5.4560
XGBoost	11	3.1799	3.1753	5.5563	5.5775
	74	2.6313	2.6129	5.4113	5.4575

Validation at 11 and 74 cumulative minutes showed that the progressive reduction in tool dimensions was captured by all three ML models. At 74 min, the measured values of 2.6313 mm and 5.4113 mm, respectively, closely matched the expected tool height (2.561–2.632 mm) and breadth (5.456–5.469 mm). All models, however, accurately depicted the basic tool-wear behavior by capturing the general declining trend in tool height and width with increasing machining time.

4.3. Volumetric Wear

The measured volume decreased from 18.5108 mm^3 at the initial condition to 17.4638 mm^3 at 11 min and 14.2061 mm^3 at 74 min. It continued to decrease at later stages, reaching 12.7263 mm^3 at 90 min, 10.0305 mm^3 at 185 min, and 6.5385 mm^3 at 205 min (Table 3 and Figure 10). Across the full sequence, the results show a progressive reduction in the reported tool-volume estimate, with the magnitude of change varying between machining stages.

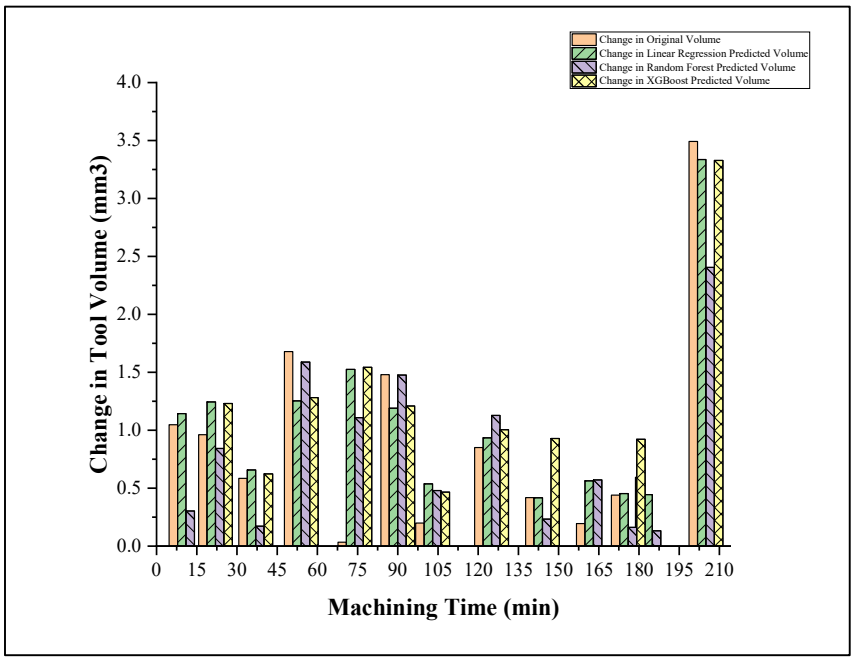


Figure 10. Prediction of change in volume.

The decreasing tool dimensions with cumulative machining time show that the proposed image-based 3D CAD reconstruction technology effectively captured progressive tool wear. Validation experiments showed that the reconstructed and measured dimensions agreed fairly well. The methodology accurately depicted total tool degradation despite differences caused by cumulative machining impacts and parameter variations. Future research will concentrate on enhancing reconstruction accuracy, extending tool wear prediction during the micromachining process utilizing the established system, and adding machining history to predictive models.

5. Conclusions

This study examined changes in USM tool geometry using microscope images, point-cloud processing, and reverse-engineering methods. The study shows that combining machine learning and image-based 3D CAD reconstruction for tool wear evaluation in ultrasonic machining is feasible. The following is a summary of the main conclusions:

(i) The developed image-based system captured dimensional changes during ultrasonic machining and effectively generated the 3D CAD model of the USM tool.

(ii) During cumulative machining, variations in power rating, abrasive slurry concentration, and flow rate affected material removal and tool wear, leading to non-uniform dimensional changes.

(iii) Promising prediction skills were shown by machine learning models; Random Forest performed best for tool width and machining volume, while Linear Regression performed best for tool height loss. Reasonable agreement with experimental measurements was validated.

(iv) Future development of automated tool wear prediction systems, dimensional monitoring, and non-contact tool condition assessment are all possible with the suggested integrated methodology.

Statement of the Use of Generative AI and AI-Assisted Technologies in the Writing Process

During the preparation of this manuscript, the authors used ChatGPT to refine and review the English. After using this tool/service, the author(s) reviewed and edited the content as needed and take(s) full responsibility for the content of the published article.

Acknowledgments

The authors gratefully acknowledge the support provided by the Department of Production Engineering, Jadavpur University.

Author Contributions

Conceptualization, A.C. and B.D.; Methodology, A.C., B.D. and K.R.; Validation, K.R. and S.S.; Formal Analysis, A.C., K.R. and J.S.; Investigation, A.C., K.R. and S.S.; Resources, B.D. and S.D.; Data Curation, A.C. and K.R.; Writing Original Draft Preparation, A.C.; Writing Review & Editing, B.D., S.D. and J.S.; Supervision, B.D.; Project Administration, A.C. All authors have read and agreed to the published version of the manuscript.

Ethics Statement

Not applicable.

Informed Consent Statement

Not applicable.

Data Availability Statement

The original data of this work is available from the corresponding author upon reasonable request.

Funding

This research received no external funding.

Declaration of Competing Interest

The authors declare that they have no known competing financial interests or personal relationships that could have appeared to influence the work reported in this paper.

References

1. Mirad MM, Das B. A critical review of the state of the art literature in the monitoring of ultrasonic machining process and tool failure prediction. *Eng. Fail. Anal.* **2021**, *130*, 105769. DOI:10.1016/j.engfailanal.2021.105769
2. Kumar S, Dvivedi A. Fabrication of microchannels using rotary tool micro-USM: An experimental investigation on tool wear reduction and form accuracy improvement. *J. Manuf. Process.* **2018**, *32*, 802–815. DOI:10.1016/j.jmapro.2018.04.008
3. Kumar S, Dvivedi A. Effect of tool materials on performance of rotary tool micro-USM process during fabrication of microchannels. *J. Braz. Soc. Mech. Sci. Eng.* **2019**, *41*, 432. DOI:10.1007/s40430-019-1922-5
4. Kumar S, Dvivedi A, Tiwari T, Tewari M. Predictive modeling of tool wear in rotary tool micro-ultrasonic machining. *Proc. Inst. Mech. Eng. Part E J. Process Mech. Eng.* **2024**, *238*, 2160–2172. DOI:10.1177/09544089231159209
5. Asmael M, Safaei B, Zeeshan Q, Zargar O, Nuhu AA. Ultrasonic machining of carbon fiber–reinforced plastic composites: A review. *Int. J. Adv. Manuf. Technol.* **2021**, *113*, 3079–3120. DOI:10.1007/s00170-021-06722-2

6. Yu Z, Ma C, An C, Li J, Guo D. Prediction of tool wear in micro USM. *CIRP Ann.* **2012**, *61*, 227–230. DOI:10.1016/j.cirp.2012.03.060
7. Wang J, Shimada K, Mizutani M, Kuriyagawa T. Tool wear mechanism and its relation to material removal in ultrasonic machining. *Wear* **2018**, *394–395*, 96–108. DOI:10.1016/j.wear.2017.10.010
8. Das S, Mazumder P, Doloi B, Bhattacharyya B. Fabricating tool for ultrasonic machining using reverse engineering. *Int. J. Comput. Integr. Manuf.* **2018**, *31*, 296–305. DOI:10.1080/0951192X.2017.1409437
9. Ferreira JC, Mateus AS, Alves NF. Rapid tooling aided by reverse engineering to manufacture EDM electrodes. *Int. J. Adv. Manuf. Technol.* **2007**, *34*, 1133–1143. DOI:10.1007/s00170-006-0690-4
10. Valerga AP, Batista M, Bienvenido R, Fernández-Vidal SR, Wendt C, Marcos M. Reverse Engineering Based Methodology for Modelling Cutting Tools. *Procedia Eng.* **2015**, *132*, 1144–1151. DOI:10.1016/j.proeng.2015.12.607
11. Che J, Zhang Y, Wang H, Liu Y, Du M, Ma S, et al. A novel method for analyzing working performance of milling tools based on reverse engineering. *J. Pet. Sci. Eng.* **2021**, *197*, 107987. DOI:10.1016/j.petrol.2020.107987
12. Cabibbo M, Forcellese A, Raffaeli R, Simoncini M. Reverse Engineering and Scanning Electron Microscopy Applied to the Characterization of Tool Wear in Dry Milling Processes. *Procedia CIRP* **2017**, *62*, 233–238. DOI:10.1016/j.procir.2016.06.087
13. Kyaw AC, Nagengast N, Usma-Mansfield C, Fuss FK. A Combined Reverse Engineering and Multi-Criteria Decision-Making Approach for Remanufacturing a Classic Car Part. *Procedia CIRP* **2023**, *119*, 222–228. DOI:10.1016/j.procir.2023.02.133
14. Azariadis P, Sapidis N. Product design using point-cloud surfaces: A recursive subdivision technique for point parameterization. *Comput. Ind.* **2007**, *58*, 832–843. DOI:10.1016/j.compind.2007.03.001
15. Motavalli S. Review of reverse engineering approaches. *Comput. Ind. Eng.* **1998**, *35*, 25–28. DOI:10.1016/S0360-8352(98)00011-4
16. Singh KJ, Ahuja IS, Kapoor J. Chemical assisted ultrasonic machining of polycarbonate glass and optimization of process parameters by Taguchi and grey relational analysis. *Adv. Mater. Process. Technol.* **2017**, *3*, 563–585. DOI:10.1080/2374068X.2017.1350022
17. Rao RV, Pawar PJ, Davim JP. Parameter Optimization of Ultrasonic Machining Process Using Nontraditional Optimization Algorithms. *Mater. Manuf. Process.* **2010**, *25*, 1120–1130. DOI:10.1080/10426914.2010.489788
18. Dvivedi A, Kumar P. Surface quality evaluation in ultrasonic drilling through the Taguchi technique. *Int. J. Adv. Manuf. Technol.* **2007**, *34*, 131–140. DOI:10.1007/s00170-006-0586-3
19. Ghosh T, Martinsen K. Generalized approach for multi-response machining process optimization using machine learning and evolutionary algorithms. *Eng. Sci. Technol. Int. J.* **2020**, *23*, 650–663. DOI:10.1016/j.jestch.2019.09.003
20. Mirad MM, Das B. Machine learning coupled with acoustic emission signal features for tool wear estimation during ultrasonic machining of Inconel 718. *Mach. Sci. Technol.* **2024**, *28*, 119–142. DOI:10.1080/10910344.2023.2299443